Chall. Nano Micro Scale Sci. Tech., 10(1): 1-13, Winter and Spring 2022
DOI: 10.22111/CNMST.2022.42130.1224

ORIGINAL RESEARCH PAPER

Acoustofluidic separation of micro and nanoparticles in Newtonian and non-Newtonian fluids: A review

Amireh Nourbakhsh*

Department of Mechanical Engineering, Bu-Ali Sina University, Hamedan, Iran

Received 17April 2022; revised 17 september 2022; accepted 13 November 2022; available online 12 March 2023

ABSTRACT: Passive and active separation of microparticles has great importance in biological analysis, diagnostics, chemical processing, etc. Acoustofluidic separation is an active technique employed to isolate or sort micron-sized particles continuously. This technique has lower power consumption compared to other active approaches. Besides, it has good biocompatibility. In this review, recent advances in acoustofluidic particle separation are discussed. Bulk Acoustic Waves (BAWs) and Surface Acoustic Waves (SAWs) are introduced and the effective forces in Newtonian and non-Newtonian fluids are defined. It is revealed that SAW transducers have several advantages for the separation of particles in comparison with BAW ones. This review demonstrates that Polydimethylsiloxane (PDMS) is widely used to fabricate microfluidic devices in which acoustic waves are employed for sorting and manipulating microparticles. Different investigations considered the separation of microparticles by acoustic waves are compared and their characteristics are determined. Besides, the challenges and perspectives of the field are analysed and discussed.

KEYWORDS: *Free vibration; MEMS; Microsensor; Modified couple stress theory; Piezoelectric; Size-dependency*

INTRODUCTION

The application of microfluidic devices has been growing due to their numerous advantages such as environmental compatibility and low cost, especially in biological utilization, in the past few years [1]. These devices have many applications in interdisciplinary science [2], chemical analysis [3], and Lab-on-a-Chip (LOC) [4] for diagnostics and engineering.

Microfluidic systems are divided into active and passive groups [5]. In active devices, an external force such as an optical field [6], acoustic field [7], magnetic field [8], etc. is employed. In passive devices, no external force is used to control particles' motion. On the other hand, the lift and drag forces cause them to move. In Newtonian fluid such as an aqueous solution, the fluid has constant viscosity. But many samples in chemical and special biological systems exhibit non-Newtonian behavior. It can say that in Newtonian fluid the inertial lift or intrinsic force becomes ineffective for small particles where the Reynolds number is less than one. But, recent studies revealed that elastic lift force for small particles in a non-Newtonian fluid or a variety of flow rates is very beneficial for manipulation. Chemical samples and biological solutions (such as DNA solutions) have non-Newtonian instincts. Besides, the suspension properties are affected by particle size and shape, solid concentration, and fluid properties. For example, spherical particles in the Newtonian fluid exhibit non-Newtonian behavior [9].

Because of the presence of non-Newtonian fluids in many industrial processes, understanding their characteristics is important [10]. Many chemical and biological samples, such as colloidal suspension and DNA solution have non-Newtonian characteristics [11]. Non-Newtonian fluids may exhibit viscoelastic behavior, which means that they behave similarly to both viscous liquid and elastic solid.

An acoustic wave propagates along a longitudinal wave and is generated by using a piezoelectric transducer. SAWs and BAWs are two kinds of acoustic waves. Standing SAWs (SSAWs) and Traveling SAWs (TSAWs) are two types of SAWs. TSAWs are the SAWs that propagate in one direction.

To generate these waves on the sides of the channel, interdigital transducer electrodes are placed [12]. SSAWs are generated by two opposite interdigitated transducers (IDTs) but TSAWs are generated by one IDT near the microchannel. BAWs propagate inside the microchannel. In this method, the piezoelectric transducer is bonded below or above the microchannel.

An alternating current (AC) power is used to generate the bulk acoustic wave because creating waves along the microchannel needs more energy than SSAWs. Figure 1 shows several devices that use various types of waves.

In TSAWs, changes in internal pressure because of the excitation of IDT on side of the microchannel move the particle [13]. In SSAWs, the position of pressure nodes and antinodes must be controlled to separate particles. The present review describes the separation of micro and nanoparticles in Newtonian and non-Newtonian fluids.

*Corresponding Author Email: *nourbakhsh@basu.ac.ir*
Tel.: +989183147941; Note. This manuscript was submitted on April 17, 2022; approved on September 17, 2022; published online March 12, 2023.

	Nomenclature		
C_D	Dean drag coefficient	$\mathbf{u}$	velocity vector (m/s)
c_0	speed of sound in fluid (m/s)	U	Average velocity (m/s)
Db	Deborah number	$\boldsymbol{v}_f$	velocity of fluid (m/s)
De	Dean number	$\boldsymbol{v}_p$	velocity of particle (m/s)
D_h	hydraulic diameter (m)	v_{rel}	relative velocity (m/s)
$e(u)$	strain rate tensor	$\forall_p$	volume of the particle (m^3)
f_1, f_2	monopole scattering coefficient	Wi	Weissenberg number
F_D	drag force (N)		**Greek Symbols**
F_{eL}	elastic force (N)	α	mobility factor
F_{iL}	Inertial force (N)	β	viscosity ratio
F^{rad}	radiation force (N)	λ	wavelength of the acoustic wave (m)
$N_1.N_2$	normal stresses (Pa)	η	dynamic viscosity (Pa.s)
p	pressure (Pa)	η_p	polymeric viscosity (Pa.s)
p_0	acoustic pressure (Pa)	ρ	density (kg/m^3)
R	curvature radius (m)	v	fluid kinematic viscosity (m^2/s)
Re_b	bulk Reynolds number	δ	thickness of the boundary layer (m)
Re_p	particle Reynolds number	ω	angular frequency of acoustic field (1/s)
t	Time (s)	ϕ	acoustophoretic contrast factor

Acoustic separation and effective forces in Newtonian and non-Newtonian fluids are discussed. Besides, different investigations performed for the manipulation or sorting of cells by using acoustic energy are provided and compared. Challenges and future directions are explained and concluding remarks are presented.

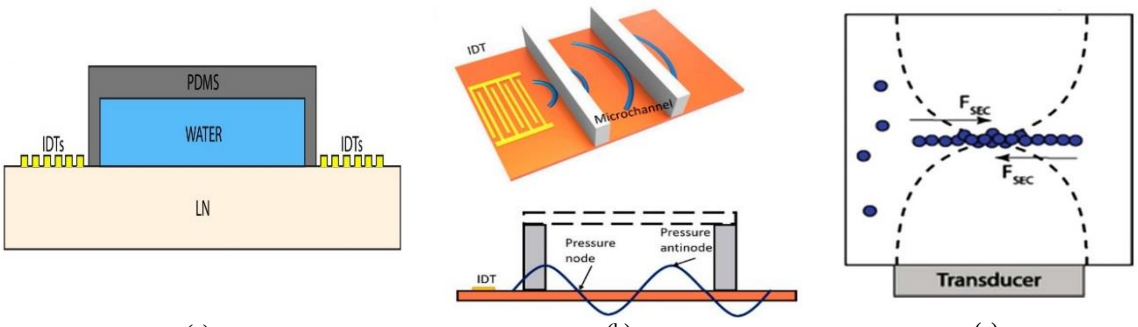

(a) (b) (c)

Fig. 1. Different methods employed to generate (a) SSAW [14], (b) TSAW [15], (c) BSW [16].

Newtonian fluids

In the microchannel, acoustic waves mostly are perpendicular to the laminar flow. The result of acoustic wave propagation is acoustic radiation force (ARF) that pushes the particles based on their size. This equation is modified for micro and nanoparticles with a radius larger than the thickness of the boundary layer δ:

$$\delta = \sqrt{2v/\omega} \tag{1}$$

where ω and v are the angular frequency of the acoustic field and fluid kinematic viscosity, respectively [17]. Governing equations for a given liquid in assumption isothermal condition are:

$$p = p(\rho) \tag{2}$$

$$\partial_t \rho = -\nabla.(\rho v) \tag{3}$$

$$\rho \partial_t v = -\nabla p - \rho(v.\nabla)v + \eta\nabla^2 v + \beta\eta\nabla(v.\nabla) \tag{4}$$

where η, β, v, p, and ρ are dynamic viscosity, the viscosity ratio, velocity field, pressure, and density, respectively [18]. The acoustic perturbation in pressure, velocity, and density is expressed as follows:

$$p = p_0 + p_1 + p_2 \tag{5a}$$
$$v = v_0 + v_1 + v_2 \tag{5b}$$
$$\rho = \rho_0 + \rho_1 + \rho_2 \tag{5c}$$

Where

$$p_1 = c_0^2 \rho_1 \tag{5d}$$

Here, $c_0 = \sqrt{(\partial p/\partial \rho)_s}$ is the speed of sound in fluid [19].

In equations 5(a-c), the first order and second order are demonstrated by subscripts 1 and 2, respectively. According to Ref. [17], the radiation force (F^{rad}) is:

$$F^{rad} = -\nabla U^{rad} \tag{6a}$$

$$U^{rad} = -\pi a^3 \left[\frac{2\kappa_0}{3} Re\{f_1^* p_1^* \nabla p_1\} - \rho_0 Re\{f_2^* v_1^*\}\right] \tag{6b}$$

$$f_1(\tilde{\kappa}) = 1 - \tilde{\kappa} \quad \text{where} \quad \tilde{\kappa} = \frac{\kappa_p}{\kappa_0} \tag{6c}$$

$$f_2(\tilde{\rho}.\tilde{\delta}) = \frac{2[1-\Gamma(\tilde{\delta})](\tilde{\rho}-1)}{2\tilde{\rho}-3\Gamma(\tilde{\delta})+1} \quad \text{where} \quad \tilde{\rho} = \frac{\rho_p}{\rho_0} \tag{6d}$$

$$\Gamma(\tilde{\delta}) = -\frac{3}{2}[1 + i(1+\tilde{\delta})]\tilde{\delta} \quad \text{where} \quad \tilde{\delta} = \frac{\delta_p}{a} \tag{6e}$$

These equations are valid for spherical particles with $a \ll \lambda$, where λ is the wavelength of the acoustic wave. f_1, and f_2 are the monopole scattering coefficient and the dipole scattering coefficient, respectively [20]. f_1 depends on the compressibility ratio and f_2 depends on the fluid viscosity [21].

The acoustic energy density is as follows:

$$E_{ac} = \frac{1}{4}\kappa_0 p_0^2 \tag{7}$$

Thus, the equation (6a) is simplified to:

$$F_{1D}^{rad} = 4\pi\phi(\tilde{\kappa}.\tilde{\rho}.\tilde{\delta})a^3 k E_{ac} sin(2ky) \tag{8a}$$

$$\phi(\tilde{\kappa}.\tilde{\rho}.\tilde{\delta}) = \frac{1}{3}f_1(\tilde{\kappa}) + \frac{1}{2}Re[f_2(\tilde{\rho}.\tilde{\delta})] \tag{8b}$$

where $\phi(\tilde{\kappa}.\tilde{\rho}.\tilde{\delta})$ is the acoustophoretic contrast factor, and $Re[f_2]$ represents the real part of f_2. This equation for a compressible particle, such as biologic cells, is [22]:

$$F_{1D}^{rad} = -\left(\frac{\pi p_0^2 \forall_p \beta_f}{2\pi}\right)\phi(\beta.\rho)sin\left(\frac{4\pi x}{\lambda}\right) \tag{9a}$$

$$\phi(\beta.\rho) = \frac{5\rho_p - \rho_f}{2\rho_p + \rho_f} - \frac{\beta_p}{\beta_f} \tag{9b}$$

where $\forall_p, p_0, \beta, \rho, \lambda$, and ϕ are the volume of the particle, acoustic pressure, compressibility, density, wavelength, and acoustic contrast factor, respectively.

Drag force

Inside a viscous fluid, as the particles move, a tensile force is applied to the particles due to the viscosity of the fluid, causing them to move along the fluid streamlines [23]. The streamlines can be used to manipulate or sort microparticles [24].

In SAWs and TSWs, acoustic streaming has an important role in separation because they create a drag force on a particle [22]. The drag force equation that acts on the particles is defined as follows:

$$F_D = -6\pi\mu r_p \boldsymbol{v}_{rel} \quad , \boldsymbol{v}_{rel} = \boldsymbol{v}_f - \boldsymbol{v}_p \tag{10}$$

where v_f and v_p represent the velocity of fluid and particle, respectively. v_{rel} is the relative velocity between particle and fluid. For small particles, the drag force can be neglected.

Total force

According to Newton's second law:

$$F = m_p \frac{d\boldsymbol{v_p}}{dt} \tag{11}$$

Two major forces acting on the particle in a microchannel with an acoustic wave field are drag force and acoustic radiation force [25]:

$$F_D + F_{ac} = m_p \frac{dv_p}{dt} \tag{12}$$

where F_D and F_{ac} were introduced in equations (10) and (6a), respectively.

In a microfluidic device that intergrades with the acoustic field, the SAW propagation is perpendicular to the flow direction, creating a pressure node at the center of the microchannel and antinodes near the walls (Figure 2).

The radiation force on a particle that acoustic waves generate moves them to a pressure node or antinode. This force relies on particle size (r_p) and acoustic contrast factor (ϕ) [26].

The sign of acoustic contrast factor specifies the direction moving of particle. In a microchannel with a positive acoustic contrast factor particles move toward pressure nodes, and if the acoustic contrast factor is a negative particle, move toward antinodes. The particle with different characteristics and acoustic properties move toward pressure nodes or antinodes [27].

Acoustic separation of particles suspended in Newtonian fluids

Manipulation of the droplets, cells, and particles has been developed by using acoustic force, leading to an interesting branch in sciences such as LOC, chemistry, and engineering. In this method, a channel that is made of a material such as silicon or glass is used for passing acoustic waves. On the other hand, these forces act on the particles in the opposite direction, and their magnitude is approximately similar. Therefore, drag force and acoustic radiation force are two main forces in the acoustic field that affect the particles. Separation particle utilizing the acoustophoretic method has several advantages such as being contactless.

Originally, particle separation by using the acoustic field is based on the interaction between particles, fluid, and acoustic waves.

Acoustic separation is due to the acoustic radiation force that affects the particles and moves them towards the side of

the microchannel. When AC power is used, waves are generated by the converter, i.e. IDT. As stated, the acoustic field can generate three kinds of waves: SSAWs, TSAWs, and BAWs. Numerous investigators utilized acoustic fields to isolate or sort microparticles/cells. For instance, Lei et al. [30] utilized a two-stage acoustic field to isolate microparticles of different sizes.

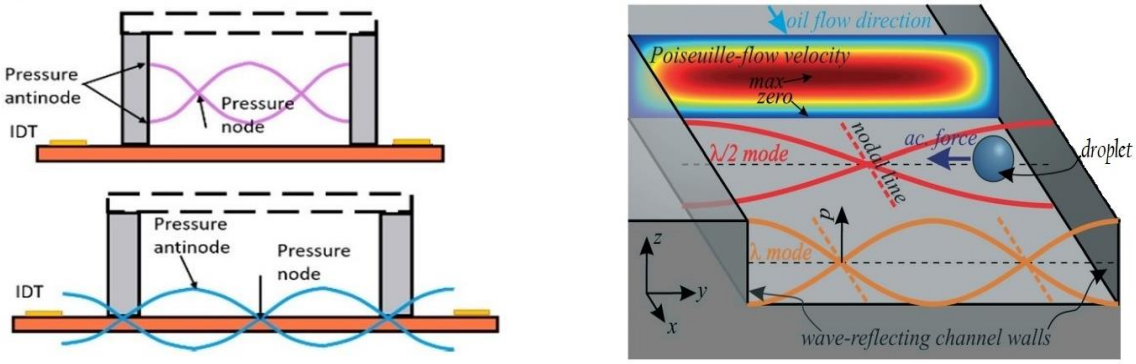

Fig. 2. (a) Position of pressure nodes and antinodes in a microchannel [28], and (b) position of pressure nodes and antinodes and direction of acoustic force [29].

They considered F_D and F_{ac} to simulate the motion of microparticles using the Gorkov and Navier-Stokes equations. 3-, 5-, and 7-μ particles were separated continuously and it was forecasted that the particles with a diameter difference of 4% can be isolated using their proposed acoustophoretic system. Vakarelski et al. [31] employed acoustic force to separate oil droplets in water experimentally by using SAWs with a frequency of 300 kHz. It was demonstrated that the acoustic contrast factor is the cause of the separation of the droplet from solid particles. Their results showed that silica particles move towards pressure nodes due to their positive acoustic contrast. These nodes were created by standing surface acoustic waves. Oil droplets moved towards the pressure antinodes due to their negative acoustic contrast. Leibacher et al. [32] used BAW acoustophoresis in a droplet microfluidic system where the acoustic frequency was about 0.1-1 MHz. They demonstrated the benefits of BAWs rather than SAWs. For example, they expressed that usually SAW devices are restricted to the piezoelectric ground plate where polydimethylsiloxane (PDMS) channels have to bond on top, but BAW devices do not have this limitation. Also, BAW devices can work under low frequencies (0.1-10 MHz), leading to longer wavelengths and the separation of larger droplets (500μm size). They reported that the BAW technique does not require electrodes and is simpler than SAW acoustophoretic system. The BAW acoustophoresis needs microchannels made of hard silicone, glass, etc. Besides, the transducer can be mounted at different distances from the channel. Friend et al. [33] reviewed the utilizations of acoustophoretic systems from the points of view of fluid mechanics and fluid dynamics. They revealed that SAW devices are easy to fabricate using planar lithography methods; hence, can be employed in many microfluidic systems. Pessôa et al. [34] investigated the magnitude of the acoustic force on arbitrary-sized spheres. They used stationary waves and Bessel beams. Their result showed that small particles are trapped due to a restoring acoustic force. Imani and Robert [35] used acoustic waves for separating particles with submicron sizes suspended in the air. The geometry of their investigation was a rectangular channel with adjustable height. The frequency of 50-80 KHz was generated by an IDT. The separation efficiency varied with the frequency of waves. Also, they observed that when the pressure of waves is increased, the separation efficiency increases and separation efficiency is higher at a lower velocity of particles. Weser et al. [36] performed an experimental analysis of the particles' lateral motion based on the acoustic fields of TSAW and SSAW using two pairs of IDTs (Figure 3) with different arrangements. Two pairs of IDTs were investigated for proving acoustic tweezers. Acoustic tweezers are tools for manipulating particles and bioparticles. Recently, using acoustic tweezers has extended for trapping and sorting particles. The application of acoustic tweezers has been developed for separating and enriching in various solutions. Guo et al. [37] presented 3D acoustic tweezers to trap nodes for manipulation. Their results showed how 3D acoustic waves can be used in the sorting and manipulation of cells. Li et al. [38] used a highly focused surface acoustic wave (HFSAW) for droplet sorting using an IDT. They observed that 51% of the initial pressure is maintained due to the fluid viscosity and the rest of the pressure could sort the particle.

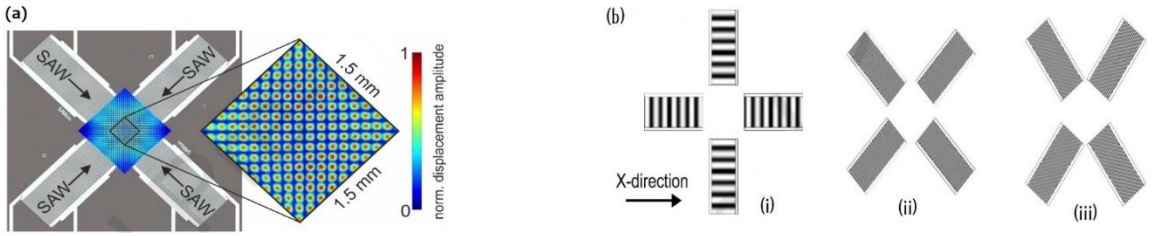

Fig. 3. (a) Schematic of SAWs in two dimensions (Acoustic tweezers), and (b) Arrangements of IDTs, (i) 0° and 90° (ii) ±45° (iii) ±52.8° [36].

Most devices designed based on BAWs have high throughput. It can be said that separation efficiency depends on several parameters, such as the channel material [39]. These devices are made of materials, such as aluminum, glass capillary tubes, or polymers. Tahmasebipour et al. [40] studied a 3D device for trapping microparticles and observed that the channel geometry and actuation can enhance the ARF. They showed that geometrical asymmetric device design has more efficiency in trapping particles. The acoustic field also reduces the formation of clogging. Deposition and accumulation of particles in a microchannel commonly occur in the colloidal fluid. This phenomenon can disrupt the flowing fluid and cause clogging. To solve this problem, Sriphutkiat and Zhou [41] proposed an acoustic method. They first simulated the effects of acoustic waves on accumulation and predict the acoustic radiation force on the particle at various viscosities. They found that using acoustic waves can decrease the accumulation region in the microchannel. Also, as the viscosity was enhanced, SSAWs reduced clogging.

Many studies have been carried out on particle separation in the oil industry, such as the extraction of oil from oily sands, the oil purification process, and the trapping of oil droplets in water [42]. For example, Hsu and Lin [43] utilized SSAWs to separate suspended microparticles of different sizes in a stagnation droplet. The frequency of their acoustic field was 30 MHz to separate 2- and 20-µm polystyrene particles. Their setup is shown in Figure 4. Input power for each IDT was 1W. ASF causes 2-µm particles to collect along with the vortex and 20-µm particles to push against the vortices of the ASF. Recently, Nazemi Ashani et al. [44] utilized two IDTs placed on a piezoelectric substrate to isolate polystyrene and polymethyl methacrylate particles and examined the impact of some effective parameters on the separation efficiency. It was found that the separation efficiency is a function of acoustic frequency and input power. They demonstrated that the separation efficiency is improved by reducing the distance between the IDTs and the channel. Optimal amounts of input power, acoustic frequency, and the distance between the IDTs and channel were reported as 1.4 W, 5 MHz, and 75 µm, respectively.

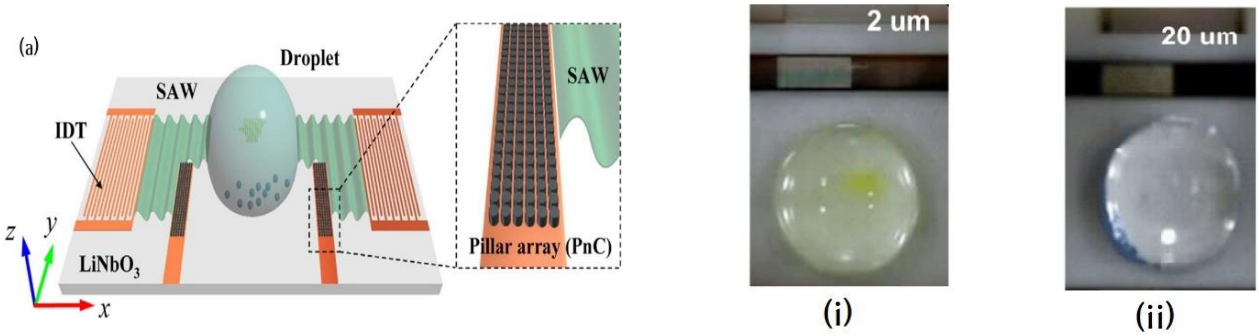

Fig. 4. (a) Schematic of the device employed to manipulate particles by using acoustic waves. (b) i: concentration of 2-µm particles, ii: concentration of 20-µm particles [43].

Commonly, the investigators set the wavelength of acoustic waves as half of the channel width when they employ SSAWs devices to create the pressure nodes on the channel walls [44]. Since smaller wavelengths result in more accurate isolation of particles, TSAWs techniques may be used. In other words, the application of TSAWs provides smaller wavelengths compared to SSAWs. On the other hand, the acoustophoresis is employed to sort or isolate microparticles when the applied frequency is kept constant. Since different modes in acoustic devices change the location of pressure nodes and antinodes, various modes may be utilized to evaluate the impact of acoustic frequency. Another crucial challenge in the field is the separation of deformable microparticles using the acoustophoretic because the migration mechanism of deformable microparticles is different when they are affected by an acoustic field.

Non-Newtonian fluids

Many chemical and biological fluids, such as plasma, saliva, hyaluronic acid (HA), and blood exhibit non-Newtonian behavior [45]. Particles in non-Newtonian fluids face several lateral forces and their direction is more

complex than in Newtonian fluids. For example, Bayareh and Mortzavi [46] studied the drop inertial migration in a shear flow. They investigated the influence of the density ratio, Reynolds number (Re), and the initial location of drops on the motion of drops in Newtonian ambient fluid and demonstrated that the equilibrium position of drops is located at the channel center. However, the motion of drops/particles is different when the surrounding fluid is non-Newtonian. Mohammadi Masiri et al. [45] utilized the Carreau-Yasuda model to simulate the motion of drops in simple shear flow and revealed that the equilibrium position of drops is changed with the amount of the relaxation time. It was reported that the drop location becomes closer to the upper wall as the relaxation time is enhanced. It can be concluded that macro and microparticles suspended in Newtonian and non-Newtonian fluids exhibit different behavior when an external actuator is applied to the channel. To evaluate the motion of the particle, continuity and momentum equations that are presented as follows, should be solved.

$$\nabla.\mathrm{u} = 0 \tag{13}$$

$$\rho\left(\frac{\partial u}{\partial t} + (u.\nabla)u\right) = \nabla.\sigma \tag{14}$$

$$\sigma = -pI + 2\eta_s e(u) + \tau \tag{15}$$

where $e(u)$ and η_s represent the strain rate tensor and viscosity of the Newtonian fluid, respectively [47]. Oldroyd-B and Giesekus equations are two viscoelastic models that can be employed as constitutive equations. The Giesekus equation is:

$$\tau + \lambda\left(\frac{\delta\tau}{\delta t} + u.\nabla\tau - \nabla u^T.\tau - \tau.\nabla u + \frac{\alpha}{\eta_p}(\tau.\tau)\right) = \eta_p(\nabla u + \nabla u^T) \tag{16}$$

where λ. η_p, α, and u are the relaxation time, polymeric viscosity, mobility factor, and velocity field, respectively. The Giesekus equations become the Oldroyd-B equation when α is zero [48]. Li et al. [49] investigated the influence of effective parameters, such as secondary flows and shear-thinning behavior in a viscoelastic fluid on sphere migration.

Karnis et al. [50] studied the axial migration of microparticles in a viscoelastic fluid (VEF). They found that the motion of particles depends on the velocity profile. Karnis and Mason [51] showed the behavior of rigid spheres, rods, disks, and liquid droplets on a micro-scale.

Due to biological applications, multiple VEF microfluidic platforms have been developed for particle manipulation and cell sorting. Yang et al. [52] proposed a method for sheath-less particle focusing, called "Elasto-Inertial Particle Focusing" in a straight microchannel. The particles, without an external force, i.e., passive technique, were aligned along the centerline of the channel under a pressure-driven flow. The passive method utilizes the geometry of the channel and properties of flow to mix different fluids or separate various particles. These techniques include pinch flow (PFF), deterministic lateral displacement (DLD), and inertial microfluidics [53-56]. Some researchers used hybrid techniques [57] by utilizing active and passive methods.

Dimensionless parameters

The dimensionless parameters that govern the motion of particles in viscoelastic fluids are as follows [58, 59]:
Elasticity number (El):

$$El = \lambda\mu/\rho H^2 \tag{17}$$

where H is the channel height.
Reynolds number (Re):

The effect of fluids on particle motion is expressed by the bulk and particle Reynolds numbers that are defined as follows, respectively.

$$Re_b = \frac{\rho U D_h}{\mu} \tag{18}$$

$$Re_p = \beta^2 Re \tag{19}$$

where D_h, U, and β are the hydraulic diameter, average velocity, and dimensionless particle blockage ratio, respectively:

$$\beta = \frac{d}{D_h} \tag{20}$$

Weissenberg number (Wi):

The viscoelastic effects are expressed by the Weissenberg number, which is the ratio of elastic force to viscous force.

$$Wi = \lambda\dot{\gamma} = \lambda\frac{2U}{D_h} \tag{21}$$

where $\dot{\gamma}$ and λ are the average fluid shear rate and the relaxation time, respectively. A large value of Wi indicates that the effects of elasticity are important.
Deborah number (Db):

$$Db = \frac{\lambda}{t_p} \tag{22}$$

Here, t_p is the characteristic time.
Dean number (De):

This number expresses the strength of flow and is written as:

$$De = Re\sqrt{\frac{D_h}{2R}} \tag{23}$$

Where R is the curvature radius (this number appears when curved microchannels are utilized).

When particles are suspended in viscoelastic fluids, two forces include lift force and drag force are applied to them due to shear stress and pressure.

Elastic lift force

This force is applied to the particle suspended in viscoelastic fluid as a result of non-uniform normal stress differences [60].

There are two normal stresses ($N_1.N_2$) exerted on the particle. For most polymer solutions that are considered as viscoelastic fluids, the magnitude of N_2 is much smaller than N_1. The use of the Oldroyd-B model leads to the following relation:

$$N_1 = -2\eta_p \lambda \dot{\gamma}^2 \tag{24}$$

Seo et al. [61] investigated the effect of different parameters on particle migration and provided the amounts of normalized $\dot{\gamma}^2$ in the microchannels cross-sections. Seo et al. [62] examined the same research on cylindrical microchannels and observed that the increment in the blockage ratio causes particles to migrate towards the tube center. When the second normal stress is negligible compared to the first one ($N_2 \ll N_1$), the magnitude of the elastic force is calculated as follows:

$$F_{eL} = C_{eL} d^3 \nabla N_1 \tag{25}$$

where C_{eL} is the non-dimensional elastic lift coefficient.

Drag force

The magnitude of the drag force is estimated by using Stokes' law [63]:

$$F_D = C_D \frac{\rho d U^2}{D_h^2 R} \tag{26}$$

where C_D is the Dean drag coefficient.

Inertial force

Because of the asymmetric distribution of vorticity around a particle, the wall-induced inertial lift (F_{iL-w}) and inertial force component (F_{iL-S}) push the particle away from the wall and the channel center, respectively [64]:

$$F_{iL} = F_{iL-w} + F_{iL-S} \tag{27}$$

$$F_{iL} = C_{iL} \rho d^4 \dot{\gamma}^2 \tag{28}$$

where C_{iL} is a non-dimensional inertial lift that is a function of particle position and *Re*. Other inertial forces that mostly can be neglected are the Magnus force and Saffman force [65].

Acoustic separation of particles suspended in non-Newtonian fluids

Particle separation and sorting in non-Newtonian fluids have significant roles in diagnostics, medical science, and health care applications. Some of these applications are the separation of biological cells, trapping circulating tumor cells (CTCs), and sorting bacteria from blood cells [66]. Active and passive methods have their advantages. Active techniques use external forces and have higher throughput and are capable of working at lower pressure differences through microchannels rather than passive techniques.

A few researchers considered viscoelastic fluids for active particle manipulation using microfluidic devices. Most of the investigators utilized inertial force as a passive technique for particle separation. Nam et al. [67] evaluated a sheathless and continuous separation of candida cells in a viscoelastic fluid. They separated 2-μm and 13-μm cells from white blood cells (WBCs) with a volume flow rate of 100 μl/min and reached a separation efficiency of 99.1%. The schematic of their device is demonstrated in Figure 5. Nikdoost and Rezai [68] examined the effects of kinematic viscosity and curvature radius on particle separation and revealed that the viscosity has a direct relation with the concentration, leading to a reduction in the *De* at a constant axial velocity. It was demonstrated that an enhancement in the channel height increases the *De*.

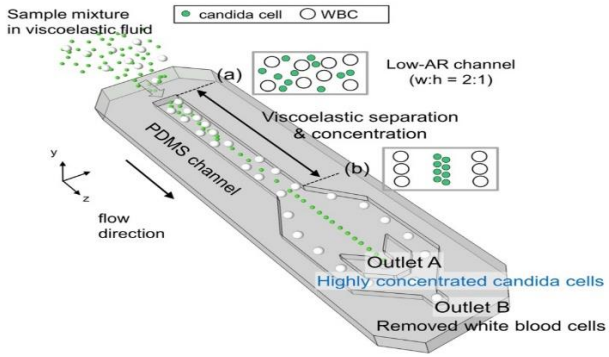

Fig. 5. Schematic of the device employed by Nam et al. [66]: (a) mixture inlet, (b) separation zone.

SSAWs are utilized in many applications, including particle sorting, particle manipulation, and droplet manipulation in medicine and biotechnology [69]. Manshadi et al. [70] reviewed the studies on the manipulation of micro and nanoparticle suspended in viscoelastic fluids and showed that acoustic waves have a simple design, high controllability, high biocompatibility, and low cost. According to the sign of acoustic contrast, particles move towards pressure nodes or antinodes created by the waves [71]. Peng et al. [72] proposed an acoustic radiation force equation as a function of several parameters such as geometric and acoustic parameters. Their equation was based on acoustic waves generated by a Gaussian ultrasound beam. They claimed that their model improves acoustic

control of drug delivery, cell trapping, cell sorting, and cell assembly. An important application of microfluidic systems with non-Newtonian fluid is their biomedical applications. Bio-liquid in the body exhibits non-Newtonian behavior [73]. Shamloo and Boodaghi [74] simulated a two-dimensional separation of red and white blood cells, and platelets from blood in a microchannel by using the finite element method (FEM) and SSAWs. The resonant frequency was 7.4125 MHz. To generate SSAWs, they used two IDTs. It was observed that the increase in the applied voltage enhances RAF. Also, they considered the effect of IDTs distance from the channel. They could separate white blood and platelets in the middle outlet and side outlets, respectively. Figure 6 shows the result of their simulations. Ren et al. [75] reported efficient cell storage based on SSAWs using a pair of IDTs.

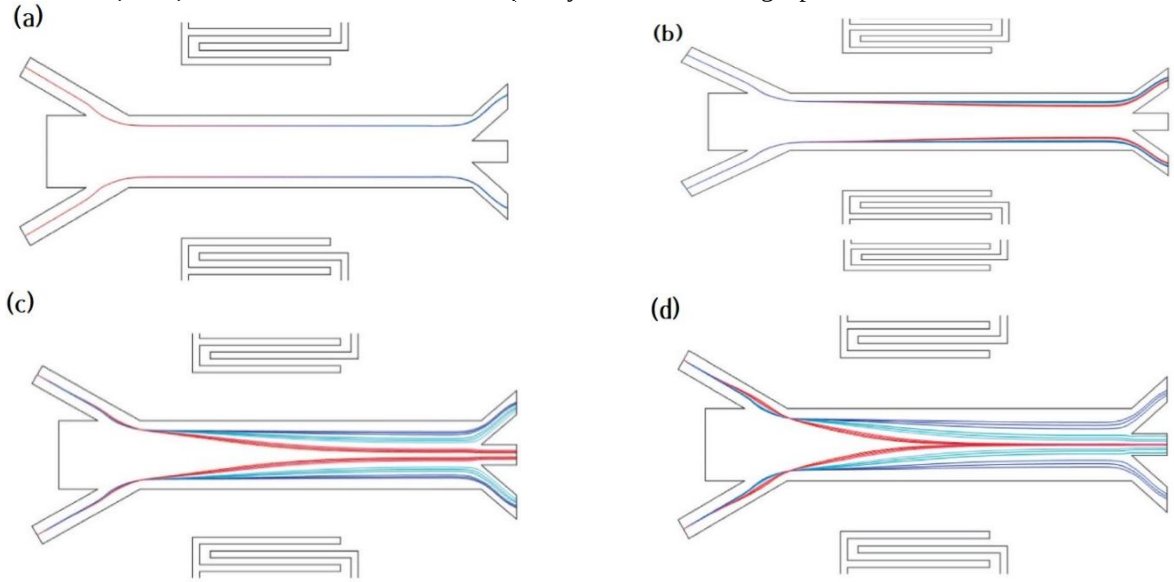

Fig. 6. Numerical simulations of Shamloo and Boodaghi [74]: (a) separation without acoustic radiation force, and separation with acoustic radiation force when the applied voltage is (b) 1V (c) 3V, and (d) 5V.

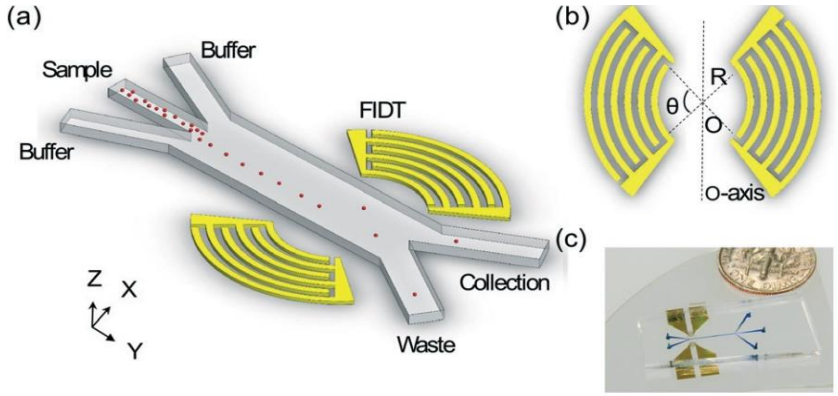

Fig. 7. (a) Schematic of device proposed by Ren et al. [75], (b) the geometry of IDTs, and (c) a picture of their device.

Their result demonstrated the storing of 10-µm polystyrene particles at 72 µs. They expressed that their device can be conveniently integrated with upstream detection units (Figure 7). Kiyasatfar and Nama [76] investigated the particle trajectories in the flow field based on the combination of acoustophoretic and electroosmotic forces and examined the effect of critical parameters such as particle size, their physical properties, input power, flow rate, and flow behavior on the particle trajectories. They stated that their model can perform as an efficient tool for quick optimizations to explore novel applications concerning the integration of electroosmotic flows with acoustofluidic technologies. Wang et al. [77] separated tumor cells from RBCs by using SAWs. They separated 2-µm and 5-µm polystyrene particles and reached an efficiency of about 94.2%. Augustsson et al. [78] developed a contactless method to separate prostate cancer cells from WBCs. They separated 5-µm microspheres from 7-µm ones with 99% purity. Ultrasonic vibration ($f_1 = 5MHz$) was applied to generate acoustic pressure nodes. The acoustic force-aligned cells are based on compressibility, density, and size. Sheidaei et al. [79] reported that the material of these devices must be suitable to reach high efficiency. The common materials used are polymeric (such as polydimethylsiloxane) or non-

polymeric (such as silicon or glass). Recently, Shiriny et al. [80] utilized inertial force to isolate microparticles in a Carreau fluid for various power-law indices and different relaxation times. They demonstrated that the Dean vortices move away from the channel center for the case of shear-thinning fluids, while they are formed in the channel centreline for a Newtonian fluid. It was found that the optimal amounts of power-law index and relaxation time is 0.7 and 0.0007 s, respectively.

other hand, more precise constitutive equations are required to model non-Newtonian fluids. Similar to the case of Newtonian fluids, the influences of deformability may be mentioned in future works.

The examination of previous investigations reveals that the manipulation of microparticles has been carried out at low amounts of *Re*. Besides, almost all researches have been performed in the suspension prepared by synthetic polymers, when the values of *Wi* are higher than *Re*. Hence, the manipulation of microparticles should be considered when the impact of elasticity and inertia is comparable. On the

A summary of the investigations on the separation, manipulation, and sorting of cells is provided in Table 1.

Table 1
Some investigations on the separation of particles using acoustic waves.

Particle type	Geometry of channel	Analysis method	Conditions and channel material	Ref.
Living and dead cells	Straight channel with 4 inlet/outlet	experimentally	Silicon and glass microchip connected to a straight channel frequency was 2MHz	[81]
Blood cells (WBCs and platelets)	Trapezoidal microchannel	Numerically Experimentally	Piezoelectric material	[82]
Micron and sub-micron particle and bovine red blood cells with E. coli	Cube channel	Experimental	Silicon and glass frequency was 2.91MHz	[83]
Polystyrene particles, Streptococcus pneumonia, and Escherichia coli	Straight channel with 3 branches at an outlet	Numerically Experimentally	Silicon and glass- frequency was 2MHz	[84]
polystyrene (PS) with 14.5 and 10μm size – sorting size base	Y Shape channel	Experimentally	polydimethylsiloxane (PDMS) channel Frequency was 13.3MHz	[85]
The particle with 2 sizes: 3.2 μm and 4.8 μm	Y Shape channel with one inlet and two outlet ports	Experimentally	tilted angle traveling surface acoustic wave – PDMS channel – frequency was 194MHz and 136MHz	[86]
blood cells and bacteria	Straight channel with 2 outlets for blood and bacteria	Experimentally	silicon chip sealed with a glass lid – frequency was 1.99MHz	[87]
purifies bacteria from the blood (include Gram-negative and -positive bacteria from blood)	the channel of the rectangular cross-section that assembled polystyrene chip and 3 outlet	Experimentally	plastic microfluidic chip – separation base on size- frequency was 1.7MHz	[88]
Polystyrene particles with diameters of 1 and 10 μm	Straight channel with 3 inlets and 2 outlet	Numerically Experimentally	The frequency was 131.83MHz Based on TSAWs waves - PDMS microchannel	[89]
two kinds of cells, MDA-MB-231 and MCF-7	Straight channel with 2 inlets and 2 outlet	Theoretically Experimentally	PDMS channel – frequency was 5MHz and 11.4MHz	[90]
multi-level sorting of polystyrene (PS) particles	with 3inlet and 3outlet in two states: Direct sorting and Sequential sorting	Numerically Experimentally	PDMS microchannel Frequency was 19.98MHz	[91]
HeLa cells with a purity ≈ 90%	Y-shaped channel	Numerically Experimentally	PDMS microchannel frequency was 200Hz	[92]
Size control of a cylindrical bubble in PDMS fluid	Cubic channel	Experimentally	PDMS channel – frequency was 21.8KHz	[93]
cellular subsets from the blood (red and white blood cells) and retrieval of breast cancer cells (MCF-7)	Straight with 3 pairs part angle of 15° relative to the main channel.	Experimentally – using acoustic stream	Silicon wafer that uses lithographic techniques	[94]

CHALLENGES AND PERSPECTIVES

Microparticles with different characteristics, including size, density, deformability, etc. can be separated by applying acoustic force. Besides, biological cells such as blood cells, CTCs, proteins, etc. are isolated by employing acoustic separation. However, acoustic chips are fabricated as PDMS using the soft lithography technique. In the future, these devices should be fabricated using plastics that are cheaper so that they can be commercialized. To prevent clogging, acoustic separation can be performed using vibration-based devices. Besides, acoustic microfluidic devices should be portable to intensify their utilization. They should be designed more simpler to reduce the fabrication cost. Acoustic chips can also be integrated with other microfluidic devices, such as micromixers and sensors, for use in various biomedical applications. Finally, particle separation in gaseous flows has been considered rarely. This subject should be contemplated in future investigations.

CONCLUSIONS

In this paper, a review of the acoustic separation technique is discussed. Acoustofluidic separation is an active method in which acoustic waves are employed to generate external force to separate particles. This technique has lower power consumption compared to other active approaches. Besides, it has good biocompatibility. The physical properties of particles determine the relationship between the main characteristics of particles and acoustic radiation force. It is revealed that SAW transducers have several advantages for the separation of particles in comparison with BAW ones. This review demonstrates that PDMS is widely used to fabricate microfluidic devices in which acoustic waves are employed for sorting and manipulating microparticles. It is found that the application of TSAWs provides smaller wavelengths compared to SSAWs. The acoustophoresis has been employed to manipulate microparticles when the applied frequency is retained constantly. It is recommended to utilize various modes to evaluate the impact of acoustic frequency. The separation of deformable microparticles suspended in Newtonian and non-Newtonian fluids using the acoustophoresis should be examined because the migration mechanism of deformable microparticles is different when they are affected by an acoustic field. For non-Newtonian cases, the manipulation of microparticles should be considered when the impact of elasticity and inertia is comparable. Finally, more precise constitutive equations are required to model non-Newtonian fluids to provide realistic models for acoustofluidic separation of microparticles.

REFERENCES

[1] Bayareh M, Nazemi Ashani M, Usefian A. Active and passive micromixers: a comprehensive review. Chemical Engineering and Processing-Process Intensification. 2020; 147: 107771.

[2] Usefian A, Bayareh M. Numerical and experimental study on mixing performance of a novel electro-osmotic micro-mixer. Meccanica. 2019; 54: 1149-1162.

[3] Hoseinpour B, Ashorynejad HR, Sarreshtehdari A. Investigation of droplet generation through Lab-On-Disk microfluidic system using Lattice Boltzmann Method. Journal of Molecular Liquids. 2021; 325: 114961.

[4] Amini H, Lee W, Di Carlo D. Inertial microfluidic physics. Lab on a Chip. 2014; 14: 2739-2761.

[5] Laurell T, Petersson F, Nilsson A. Chip integrated strategies for acoustic separation and manipulation of cells and particles. Chemical Society Reviews. 2007; 36: 492-506.

[6] Sancho-Fornes G, Avella-Oliver M, Carrascosa J, Fernandez E, Brun EM, Maquieira A. Disk-based one-dimensional photonic crystal slabs for label-free immunosensing. Biosensors and Bioelectronics. 2019; 126: 315-323.

[7] Ghorbani Kharaji Z, Bayareh M, Kalantar V. A review on acoustic field-driven micromixers. International Journal of Chemical Reactor Engineering. 2021; 19(6): 553-569.

[8] Shiriny A, Bayareh M. On magnetophoretic separation of blood cells using Halnach array of magnets. Meccanica. 2020; 55: 1903-1916.

[9] Mer OS, Rui L, Yulin D. Microfluidic Approaches for Cancer Cell Separation. Journal of Biomedical Science and Engineering. 2014; 7: 1005-1018.

[10] Nguyen N-T, Wereley ST, Shaegh SAM. Fundamentals and applications of microfluidics: Artech house. 2019.

[11] Bayareh M. An updated review on particle separation in passive microfluidic devices. Chemical Engineering and Processing-Process Intensification. 2020; 153: 107984.

[12] Sande MG, Çaykara T, Silva CJ, Rodrigues LR. New solutions to capture and enrich bacteria from complex samples. Medical Microbiology and Immunology. 2020; 209: 1-7.

[13] Yan S, Yuan D. Continuous microfluidic 3D focusing enabling microflow cytometry for single-cell analysis. Talanta. 2021; 221: 121401.

[14] Lenshof A, Evander M, Laurell T, Nilsson J. Acoustofluidics 5: Building microfluidic acoustic resonators. Lab on a Chip. 2012; 12: 684-695.

[15] Augustsson P, Barnkob R, Wereley ST, Bruus H, Laurell T. Automated and temperature-controlled micro-PIV measurements enabling long-term-stable microchannel acoustophoresis characterization. Lab on a Chip. 2011; 11: 4152-4164.

[16] Ai Y, Sanders CK, Marrone BL. Separation of Escherichia coli bacteria from peripheral blood mononuclear cells using standing surface acoustic waves. Analytical chemistry. 2013; 85: 9126-9134.

[17] Liu G, He F, Li X, Zhao H, Zhang Y, Li Z, Yang Z. Multi-level separation of particles using acoustic

radiation force and hydraulic force in a microfluidic chip. Microfluidics and Nanofluidics. 2019; 23: 23.
[18] Gao Y, Wu M, Lin Y, Xu J. Acoustic Microfluidic Separation Techniques and Bioapplications: A Review. Micromachines. 2020; 11: 921.
[19] Trujillo FJ, Juliano P, Barbosa-Cánovas G, Knoerzer K. Separation of suspensions and emulsions via ultrasonic standing waves–A review. Ultrasonics sonochemistry. 2014; 21: 2151-2164.
[20] Landau L, Lifshitz EM. Fluid Mechanics. Course of theoretical physics. 1959; 6.
[21] Settnes M, Bruus H. Forces acting on a small particle in an acoustical field in a viscous fluid. Physical Review E. 2012; 85: 016327.
[22] Doinikov AA. Acoustic radiation force on a spherical particle in a viscous heat-conducting fluid. II. Force on a rigid sphere. The Journal of the Acoustical Society of America. 1997; 101: 722-730.
[23] Sriphutkiat Y, Zhou Y. Particle accumulation in a microchannel and its reduction by a standing surface acoustic wave (SSAW). Sensors. 2017; 17: 106.
[24] Sivaramakrishnan M, Kothandan R, Govindarajan DK, Meganathan Y, Kandaswamy K. Active microfluidic systems for cell sorting and separation. Current Opinion in Biomedical Engineering. 2020; 13: 60-68.
[25] Karle M, Vashist SK, Zengerle R, von Stetten F. Microfluidic solutions enabling continuous processing and monitoring of biological samples: A review. Analytica Chimica Acta. 2016; 929: 1-22.
[26] Manoorkar S, Morris JF. Particle motion in pressure-driven suspension flow through a symmetric T-channel. International Journal of Multiphase Flow. 2021; 134: 103447.
[27] Manasseh R. Acoustic bubbles, acoustic streaming, and cavitation microstreaming. Handbook of Ultrasonics and Sonochemistry. 2016; 33.
[28] Augustsson P, Magnusson C, Nordin M, Lilja H, Laurell T. Microfluidic, label-free enrichment of prostate cancer cells in blood based on acoustophoresis. Analytical chemistry. 2012; 84: 7954-7962.
[29] Ozcelik A, Rufo J, Guo F, Gu Y, Li P, Lata J, Huang TJ. Acoustic tweezers for the life sciences. Nature methods. 2018; 15: 1021-1028.
[30] Lei J, Cheng F, Li K, Guo Z. Numerical simulation of continuous separation of microparticles in two-stage acousto-microfluidic systems. Applied Mathematical Modelling. 2020; 83: 342-356.
[31] Vakarelski IU, Li EQ, Abdel-Fattah AI, Thoroddsen ST. Acoustic separation of oil droplets, colloidal particles and their mixtures in a microfluidic cell. A Physicochemical and engineering aspects. 2016; 506: 138-147.
[32] Leibacher I, Reichert P, Dual J. Microfluidic droplet handling by bulk acoustic wave (BAW) acoustophoresis. Lab on a Chip. 2015; 15: 2896-2905.
[33] Friend J, Yeo LY. Microscale acoustofluidics: Microfluidics driven via acoustics and ultrasonics. Reviews of Modern Physics. 2011; 83: 647.
[34] Pessôa MAS, Neves AAR. Acoustic scattering and forces on an arbitrarily sized fluid sphere by a general acoustic field. Journal of Sound and Vibration. 2020; 479: 115373.
[35] Imani RJ, Robert E. Acoustic separation of submicron solid particles in air. Ultrasonics. 2015; 63: 135-140.
[36] Weser R, Winkler A, Weihnacht M, Menzel S, Schmidt H. The complexity of surface acoustic wave fields used for microfluidic applications. Ultrasonics. 2020; 106: 106160.
[37] Guo F, Mao Z, Chen Y, Xie Z, Lata JP, Li P, Ren L, Liu J, Yang J, Dao M, Suresh S, Huang TJ. Three-dimensional manipulation of single cells using surface acoustic waves. Proceedings of the National Academy of Sciences. 2016; 113: 1522-1527.
[38] Li P, Ma Z, Zhou Y, Collins DJ, Wang Z, Ai Y. Detachable acoustophoretic system for fluorescence-activated sorting at the single-droplet level. Analytical chemistry. 2019; 91: 9970-9977.
[39] Gautam GP, Burger T, Wilcox A, Cumbo MJ, Graves SW, Piyasena ME. Simple and inexpensive micromachined aluminum microfluidic devices for acoustic focusing of particles and cells. Analytical and bioanalytical chemistry. 2018; 410: 3385-3394.
[40] Tahmasebipour A, Friedrich L, Begley M, Bruus H, Meinhart C. Toward optimal acoustophoretic microparticle manipulation by exploiting asymmetry. The Journal of the Acoustical Society of America. 2020; 148: 359-373.
[41] Sriphutkiat Y, Zhou Y. Particle Accumulation in a Microchannel and Its Reduction by a Standing Surface Acoustic Wave (SSAW). Sensors. 2017; 17(12): 106.
[42] Xie W, Li R, Lu X. Pulsed ultrasound assisted dehydration of waste oil. Ultrasonics sonochemistry. 2015; 26: 136-141.
[43] Hsu JC, Lin YD. Microparticle concentration and separation inside a droplet using phononic-crystal scattered standing surface acoustic waves. Sensors and Actuators A: Physical. 2019; 300: 111651.
[44] Nazemi Ashani M, Bayareh M, Ghasemi B. Acoustofluidic separation of microparticles: a numerical study. Iranian Journal of Chemistry and Chemical Engineering. 2022. 10.30492/ijcce.2021.535756.4876.
[45] Mohammadi Masiri S, Bayareh M, Ahmadi Nadooshan A. Pairwise interaction of drops in shear-thinning inelastic fluids. Korea-Australia Rheology Journal. 2019; 31: 25-34, http://dx.doi.org/10.1007/s13367-019-0003-8.
[46] Bayareh M, Mortazavi S. Effect of density ratio on the hydrodynamic interaction between two drops in simple shear flow. Iranian Journal of Science and Technology. 2011; 35: 121-132.

[47] Bhat PP, Appathurai S, Harris MT, Pasquali M, McKinley GH, Basaran OA. Formation of beads-on-a-string structures during break-up of viscoelastic filaments. Nature Physics. 2010; 6: 625-631.
[48] Graham MD. Fluid dynamics of dissolved polymer molecules in confined geometries. Annual Review of Fluid Mechanics. 2011; 43: 273-298.
[49] Li H, Ku X, Lin J. Eulerian–Lagrangian simulation of inertial migration of particles in circular Couette flow. Physics of Fluids. 2020; 32: 073308.
[50] Karnis A, Goldsmith H, Mason S. Axial migration of particles in Poiseuille flow. Nature. 1963; 200: 159-160.
[51] Karnis A, Mason S. Particle motions in sheared suspensions. XIX. Viscoelastic media. Transactions of the Society of Rheology. 1966; 10: 571-592.
[52] Yang S, Kim JY, Lee SJ, Lee SS, Kim JM. Sheathless elasto-inertial particle focusing and continuous separation in a straight rectangular microchannel. Lab on a Chip. 2011; 11: 266-273.
[53] Usefian A, Bayareh M, Ahmadi Nadooshan A. Rapid mixing of Newtonian and non-Newtonian fluids in a three-dimensional micro-mixer using non-uniform magnetic field. Journal of Heat and Mass Transfer Research. 2019; 6(1): 56-61.
[54] Usefian A, Bayareh M. Numerical and experimental investigation of an efficient convergent–divergent micromixer. Meccanica. 2020; 55: 1025-1035.
[55] Bayareh M. Artificial diffusion in the simulation of micromixers: A review. Proceedings of the Institution of Mechanical Engineers, Part C: Journal of Mechanical Engineering Science. 2020; 235: 5288-5296.
[56] Shiriny A, Bayareh M. Inertial focusing of CTCs in a novel spiral microchannel. Chemical Engineering Science. 2020; 229: 116102.
[57] Shiriny A, Bayareh M, Ahmadi Nadooshan A. Combination of inertial focusing and magnetoporetic separation in a novel microdevice. Korean Journal of Chemical Engineering. 2021; 38(8): 1686-1702.
[58] D'Avino G, Maffettone PL. Particle dynamics in viscoelastic liquids. Journal of Non-Newtonian Fluid Mechanics. 2015; 215: 80-104.
[59] Del Giudice F, D'Avino G, Greco F, Netti PA, Maffettone PL. Effect of fluid rheology on particle migration in a square-shaped microchannel. Microfluidics and Nanofluidics. 2015; 19: 95-104.
[60] Browne CA, Shih A, Datta SS. Pore Scale Flow Characterization of Polymer Solutions in Microfluidic Porous Media. Small. 2020; 16: 1903944.
[61] Seo KW, Kang YJ, Lee SJ. Lateral migration and focusing of microspheres in a microchannel flow of viscoelastic fluids. Physics of Fluids. 2014; 26: 063301.
[62] Seo KW, Byeon HJ, Huh HK, Lee SJ. Particle migration and single-line particle focusing in microscale pipe flow of viscoelastic fluids. RSC advances. 2014; 4: 3512-3520.
[63] Villone M, D'avino G, Hulsen M, Greco F, Maffettone P. Particle motion in square channel flow of a viscoelastic liquid: Migration vs. secondary flows. Journal of Non-Newtonian Fluid Mechanics. 2013; 195: 1-8.
[64] Zhang J, Yan S, Yuan D, Alici G, Nguyen NT, Warkiani ME, Li W. Fundamentals and applications of inertial microfluidics: a review. Lab on a Chip. 2016; 16: 10-34.
[65] Martel JM, Toner M. Inertial focusing in microfluidics. Annual review of biomedical engineering. 2014; 16: 371-396.
[66] Lim H, Back SM, Hwang MH, Lee DH, Choi H, Nam J. Sheathless high-throughput circulating tumor cell separation using viscoelastic non-newtonian fluid. Micromachines. 2019; 10: 462.
[67] Nam J, Jang WS, Lim CS. Viscoelastic separation and concentration of fungi from blood for highly sensitive molecular diagnostics. Scientific reports. 2019; 9: 1-12.
[68] Nikdoost A, Rezai P. Dean flow velocity of viscoelastic fluids in curved microchannels. AIP Advances. 2020; 10: 085015.
[69] Wang K, Zhou W, Lin Z, Cai F, Li F, Wu J, Meng L, Niu L, Zheng H. Sorting of tumour cells in a microfluidic device by multi-stage surface acoustic waves. Sensors and Actuators B: Chemical. 2018; 258: 1174-1183.
[70] Manshadi MK, Mohammadi M, Monfared LK, Sanati-Nezhad A. Manipulation of micro-and nanoparticles in viscoelastic fluid flows within microfluid systems. Biotechnology and Bioengineering. 2020; 117: 580-592.
[71] Barani A, Paktinat H, Janmaleki M, Mohammadi A, Mosaddegh P, Fadaei-Tehrani A, Sanati-Nezhad A. Microfluidic integrated acoustic waving for manipulation of cells and molecules. Biosensors and Bioelectronics. 2016; 85: 714-725.
[72] Peng X, He W, Xin F, Genin GM, Lu TJ. The acoustic radiation force of a focused ultrasound beam on a suspended eukaryotic cell. Ultrasonics. 2020; 108: 106205.
[73] De Cock I, Zagato E, Braeckmans K, Luan Y, de Jong N, De Smedt SC, Lentacker I. Ultrasound and microbubble mediated drug delivery: acoustic pressure as determinant for uptake via membrane pores or endocytosis. Journal of controlled release. 2015; 197: 20-28.
[74] Shamloo A, Boodaghi M. Design and simulation of a microfluidic device for acoustic cell separation. Ultrasonics. 2018; 84: 234-243.
[75] Ren L, Chen Y, Li P, Mao Z, Huang PH, Rufo J, Guo F, Wang L, McCoy JP, Levine SJ, Huang TJ. A high-throughput acoustic cell sorter. Lab on a Chip. 2015; 15: 3870-3879.

[76] Kiyasatfar M, Nama N. Particle manipulation via integration of electroosmotic flow of power-law fluids with standing surface acoustic waves (SSAW). Wave Motion. 2018; 80: 20-36.
[77] Wang K, Zhou W, Lin Z, Cai F, Li F, Wu J, Meng L, Niu L, Zheng H. Sorting of tumour cells in a microfluidic device by multi-stage surface acoustic waves. Sensors and Actuators B: Chemical. 2018; 258: 1174-1183.
[78] Augustsson P, Magnusson C, Nordin M, Lilja H, Laurell T. Microfluidic, label-free enrichment of prostate cancer cells in blood based on acoustophoresis. Analytical chemistry. 2012; 84: 7954-7962.
[79] Sheidaei Z, Akbarzadeh P, Kashaninejad N. Advances in numerical approaches for microfluidic cell analysis platforms. Journal of Science: Advanced Materials and Devices. 2020; 5(3): 295-307.
[80] Shiriny A, Bayareh M, Usefian A. Inertial separation of microparticles suspended in shear-thinning fluids. Chem Pap. 2022; 76: 4341–4350, https://doi.org/10.1007/s11696-022-02184-2.
[81] Olofsson K, Hammarström B, Wiklund M. Acoustic separation of living and dead cells using high density medium. Lab on a Chip. 2020; 20: 1981-1990.
[82] Shamloo A, Parast FY. Simulation of blood particle separation in a trapezoidal microfluidic device by acoustic force. IEEE Transactions on Electron Devices. 2019; 66: 1495-1503.
[83] Gautam GP, Gurung R, Fencl FA, Piyasena ME. Separation of sub-micron particles from micron particles using acoustic fluid relocation combined with acoustophoresis. Analytical and bioanalytical chemistry. 2018; 410: 6561-6571.
[84] Van Assche D, Reithuber E, Qiu W, Laurell T, Henriques-Normark B, Mellroth P, Ohlsson P, Augustsson P. Gradient acoustic focusing of sub-micron particles for separation of bacteria from blood lysate. Scientific reports. 2020; 10: 1-13.
[85] Simon G, Pailhas Y, Andrade MA, Reboud J, Marques-Hueso J, Desmulliez MP, Cooper JM, Riehle MO, Bernassau AL. Particle separation in surface acoustic wave microfluidic devices using reprogrammable, pseudo-standing waves. Applied Physics Letters. 2018; 113: 044101.
[86] Ahmed H, Destgeer G, Park J, Afzal M, Sung HJ. Sheathless focusing and separation of microparticles using tilted-angle traveling surface acoustic waves. Analytical chemistry. 2018; 90: 8546-8552.
[87] Ohlsson P, Petersson K, Augustsson P, Laurell T. Acoustic impedance matched buffers enable separation of bacteria from blood cells at high cell concentrations. Scientific reports. 2018; 8: 1-11.
[88] Dow P, Kotz K, Gruszka S, Holder J, Fiering J. Acoustic separation in plastic microfluidics for rapid detection of bacteria in blood using engineered bacteriophage. Lab on a Chip. 2018; 18: 923-932.
[89] Liu G, Li Z, Li X, Li Y, Tang H, Wang M, Yang Z. Design and experiment of a focused acoustic sorting chip based on TSAW separation mechanism. Microsystem Technologies. 2020; 26(9): 1-12.
[90] Meng L, Cui X, Dong C, Liu X, Zhou W, Zhang W, Wang X, Niu L, Li F, Cai F, Wu J, Zheng H. Microbubble enhanced acoustic tweezers for size-independent cell sorting. Applied Physics Letters. 2020; 116: 073701.
[91] Liu G, et al. Effects of two surface acoustic wave sorting chips on particles multi-level sorting Biomedical microdevices. 2019; 21(3): 59.
[92] Ren L, et al. Standing Surface Acoustic Wave (SSAW)-Based Fluorescence-Activated Cell Sorter. Small. 2018; 14(40): 1801996.
[93] Volk A, Kähler CJ. Size control of sessile microbubbles for reproducibly driven acoustic streaming. Physical Review Applied. 2018; 9: 054015.
[94] Garg N, Westerhof TM, Liu V, Liu R, Nelson EL, Lee AP. Whole-blood sorting, enrichment and in situ immunolabeling of cellular subsets using acoustic microstreaming. Microsystems & Nanoengineering. 2018; 4: 1-9.